

# Testing the effect of geodesic mixing with COBE data to reveal the curvature of the universe

V.G. Gurzadyan<sup>1,\*</sup> and S. Torres<sup>2</sup>

<sup>1</sup> University of Sussex, Brighton, UK; Dept. of Theoretical Physics, Yerevan Physics Institute, 375036, Yerevan, Armenia (permanent address)

<sup>2</sup> Observatorio Astronómico Nacional, Universidad Nacional de Colombia, and Centro Internacional de Física, Bogotá, Colombia

Received 21 March 1996 / Accepted 2 October 1996

**Abstract.** When considering the statistical properties of a bundle of cosmic microwave background (CMB) photons propagating through space, the effect of ‘mixing geodesics’ appears with a distinct signature that depends on the geometry of space. In a Universe with negative curvature this effect is expected to produce elongated anisotropy spots on CMB maps. We used COBE-DMR data to look for such effect. Based on the analysis of a measure of eccentricity of hot spots it appears that there is a clear indication of an excess eccentricity of hot spots with respect to that expected from noise alone. This result must be interpreted with caution as this effect can be due in part to galactic emission. If the detected eccentricity of anisotropy spots can be attributed to the effect of mixing it implies the negative curvature of the Universe and a value of  $\Omega < 1$ .

**Key words:** cosmic microwave background – cosmology: theory; observations

---

## 1. Introduction

The detection (Smoot et al. 1992; Bennett et al. 1994) and further confirmation (Bennett et al. 1996; Hancock et al. 1994; Ganga et al. 1993) of the presence of anisotropies in the cosmic microwave background (CMB), has endowed cosmologists with a unique tool for a realistic test of cosmological models. The observed large angle  $\Delta T/T$  can be produced by a number of sources that go from local, to astrophysical, to cosmological effects, among which the most relevant are: emission from the Galaxy; gravitational fluctuations produced by voids and great attractors; the Doppler effect due to the observer’s motion relative to the CMB; mixing of geodesic flow; gravitational waves; cosmic strings; and gravitational potential fluctuations on the last scattering surface – the Sachs-Wolfe effect (for a review

see White, Scott & Silk 1994). Clearly the complexity of determining the cause of CMB anisotropies requires several independent analysis techniques. Aside from the standard statistical tests based on the angular auto-correlation function and power spectrum, a number of statistics have been proposed (Sazhin 1985; Vittorio & Juszkiewicz 1987; Bond & Efstathiou 1987; Coles 1988; Gott et al. 1990; Martínez-González & Cayón 1992; Martínez-González & Sanz 1989) as topological descriptors to characterize the observed anisotropies: hot spot number density, length and total curvature or *genus* of iso-temperature contours, number of upcrossings, area and eccentricity of hot spots, and Euler-Poincaré characteristic. The study of these topological descriptors is based on the well established theory of the geometric properties of the excursion set of random fields (Adler 1981).

The great potential of topological analysis of CMB data can be attested by the large number of results obtained thus far: the *genus* descriptor has been successfully used to place important restrictions on the shape of the spectrum of primordial perturbations  $P(k)$  (Smoot et al. 1994; Torres 1994; Torres 1995a; Torres et al. 1995); further restrictions on  $P(k)$  have been obtained from the peak distribution analysis (Fabbri & Torres 1995, 1996); a possible fractal dimension in the universe has been detected with the analysis of the contour characteristics of anisotropy spots (De Gouveia 1995); studies of hot spot number density (Torres 1995b; Cayón & Smoot 1995) support the results given by the *genus* analysis; tests of Gaussianity of the CMB field have been performed using the *genus* and the correlation function of local maxima (Kogut et al. 1996); finally, percolation and cluster analysis (Naselsky & Novikov 1995) of CMB maps has been proposed as a powerful tool to test the Gaussian character of CMB anisotropies. The information carried by the CMB properties can even have a direct impact on accelerator physics (Gurzadyan & Margarian 1996).

We propose to use a topological analysis, based on the eccentricity or elongation measure of hot spots, to look for the signature of the mixing of geodesics effect (Gurzadyan & Kocharyan 1991, 1992). Because of the appealing possibility of extracting information about the curvature of the universe from the latter

---

Send offprint requests to: V.G. Gurzadyan

\* Affiliated to ICRA

effect, we will deal with it in some detail. A consequence of mixing phenomena in geodesics propagation is the appearance of highly distorted anisotropy spots in cosmic background maps (Gurzadyan & Kocharyan 1993a, 1993b). In the case of an open geometry, anisotropy spots associated with a bundle of photons propagating in free space would appear as highly elongated hot spots, while in a flat space hot spots would show a symmetric circular shape. This visible effect is a direct consequence of the geometry of space and as such it is a unique tool to discriminate between open and closed cosmological models. However, confusion due to galactic contamination at high latitudes and similar elongated patterns produced by instrumental noise and cosmological structure characterized by large coherence angles makes this effect very difficult to observe.

Fortunately, at least 3 different phenomena produced by the effect of mixing geodesics and associated with the observable characteristics of CMB, have been predicted:

(a) *Isotropization*. The decrease of the amplitude of CMB anisotropy after the decoupling epoch: the degree of isotropization, i.e. the fluctuation damping factor can yield up to  $10^3$  for  $\Omega = 0.2-0.4$  (Gurzadyan & Kocharyan 1991,1992)<sup>1</sup>;

(b) *Angular dependence*. The behaviour of anisotropy as a function of the sky and smoothing (beam) angles, namely, the independence of the autocorrelation function on the sky angle, and its dependence on the smoothing angle (Gurzadyan & Kocharyan 1996);

(c) *Maps*. The complex topological structure of the CMB sky maps, showing intrinsic *threshold independent* elongation of the shapes of both hot and cold spots (Gurzadyan & Kocharyan 1993a, 1993b).

In this paper we will deal only with the third phenomenon. Since, in principle, effects of apparent elongation might occur also owing to other physical mechanisms (the same is not excluded also for phenomena (a) and (b)), the unambiguous confirmation of the observational discovery of the effect of mixing geodesics could be reached by means of a comprehensive study of the complete set of predictions. As it is briefly discussed at the end of this paper, at least the available evidences do not contradict to all these predictions. A confirmation of the effect of mixing geodesics would constitute powerful probe of the curvature of the Universe.

## 2. Effect of mixing of geodesics flow: maps

The idea of the effect of instability of trajectories of freely moving particles can be most clearly demonstrated via the Jacobi equation written for spaces with constant curvature  $k$ :

$$d^2 \mathbf{n} / d^2 \lambda + k \mathbf{n} = 0, \quad (1)$$

describing the behavior of the vector of deviation,  $\mathbf{n}$ , of close geodesics. Solutions of this equation are determined by the sign

<sup>1</sup> In Eq(12) of the interesting paper by Ellis and Tavakol (1994) an additional numerical factor 2 is necessary, as readily follows from Pesin's theorem; in the rest those authors indeed confirm the above mentioned results on the decrease of CMB anisotropy via geodesic mixing.

of the curvature: when  $k < 0$  one has exponentially deviating geodesics.

A more rigorous treatment (Gurzadyan & Kocharyan 1991, 1992) includes the study of the projection of geodesics from (3+1)-dimensional Lorentzian space to a 3D Riemannian one, and the behavior of time correlation functions for geodesic flows on homogeneous isotropic spaces with negative curvature. Geodesic flows, being Anosov systems (locally if the space is not compact), are exponentially unstable systems possessing: the strongest statistical properties (mixing), non-zero Lyapunov characteristic exponents, and positive Kolmogorov-Sinai (KS) entropy  $h$  (Arnold 1989).

For Anosov systems two geodesics in 3-space deviate exponentially according to the law

$$\mathbf{n}(\lambda) = \mathbf{n}(0) \exp(\chi \lambda), \quad (2)$$

where  $\chi$  is the Lyapunov exponent.

For a homogeneous isotropic Friedmannian Universe with  $k = -1$  the Lyapunov exponent is determined by the only parameter  $a$ , the diameter of the Universe:

$$\chi = 1/a, \quad (3)$$

while Lyapunov exponents vanish when  $k = 0, +1$ .

Time correlation functions, describing the decrease of perturbations also decay exponentially as determined by KS-entropy:  $h = 2\chi$ .

For the Universe expanding as

$$a(t) = a(t_0)(t/t_0)^\alpha, \quad (4)$$

the relation between the quantitative measurement of the distortion of patterns,  $\epsilon$ , and  $\Omega$  is given by (Gurzadyan & Kocharyan 1993):

$$\frac{\ln(1/\epsilon)}{\left(\frac{1-\Omega_0}{1+z\Omega_0}\right)^{\frac{1}{2}}} = \begin{cases} \alpha/(1-\alpha)[1 - (1+z_1)^{1-1/\alpha}] & \alpha < 1 \\ \ln(1+z_1) & \alpha = 1 \end{cases} \quad (5)$$

where  $\Omega_0$  is its present value ( $z = 0$ ),  $z_1$  corresponds to the time when matter becomes non relativistic and  $z(\approx 1000)$  to the decoupling time. We deliberately used the power law representation for the expansion law, (instead of trivial use of the corresponding exact Einstein equation) to demonstrate the role of the expansion rate in the described effect. It is not excluded that in the future the geodesic mixing effect can be useful to gain information also on the expansion rate of the Universe after the decoupling epoch.

The parameter of elongation  $\epsilon$  defined via the divergence of geodesics in (3+1)-space:

$$\epsilon = \frac{l(t)}{l(0)}, \quad l(t) = l(t_0) \frac{a(t)}{a(t_0)} \exp(\chi \lambda(t)), \quad (6)$$

approaches 1 when  $\Omega$  tends to 1 as shown in Fig. 1.

The typical pattern of a hot spot as seen today in a  $k < 1$  universe would exhibit a very complex shape. The elongation,  $\epsilon$ , measures the smallest-to-largest ratio of diameters of one-connected regions and is related to the "degree of complexity" of anisotropies.

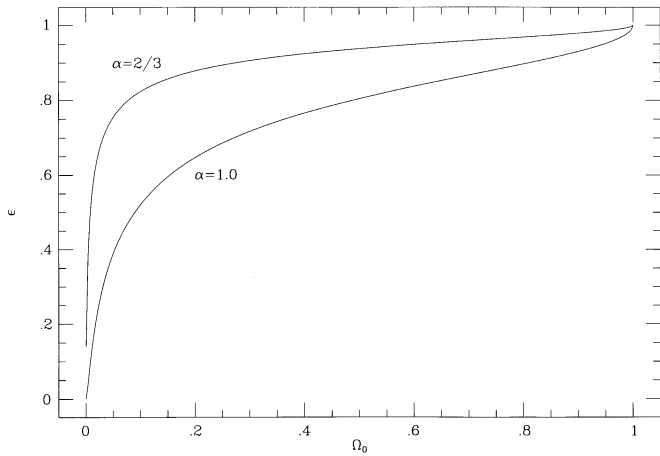


**Fig. 1.** Elongation parameter  $\epsilon$  as a function of  $\Omega$  for two exponents for the law of the expansion rate of the Universe,  $\alpha = 1$  and  $\alpha = 2/3$ .

### 3. Analysis of DMR maps

COBE's Differential Microwave Radiometers (DMR) have mapped the microwave sky at three frequencies: 31, 53, and 90 GHz (Smoot et al. 1990). The analysis presented here is based on DMR's 53 GHz maps (which have the best sensitivity) of the four year data set (Bennett et al. 1996), and is a continuation of the study based on the one year data-set (Gurzadyan & Torres 1993). Signal and noise maps were prepared by adding and subtracting the two independent DMR channels (ie.  $0.5A + 0.5B$  and  $0.5A - 0.5B$ ) and Gaussian smoothing ( $\sigma = 2.9^\circ$ ) the resulting maps. A Galaxy cut  $|b| < 20^\circ$  has been applied to the maps. The geometric characteristics of hot spots are quite sensitive to galactic cuts below  $15^\circ$  to  $20^\circ$  but beyond  $20^\circ$  our results are stable.

DMR maps are digitized on a grid of 6144 approximately equal area pixels of size  $\sim 2.9^\circ$  (Torres et al. 1989). A hot spot is defined as a continuous region of the map formed by pixels whose temperature is higher than a preset threshold  $T_\nu = \nu\sigma$ , where  $\sigma$  is the standard deviation of the sky temperature (monopole and dipole subtracted). The algorithm to identify hot spots (Torres 1994, Torres 1995a) relies on the construction of binary tree structures out of the set of connected 'hot' pixels (for a given temperature threshold). The number of pixels in a tree gives the area of the spot. The eccentricity parameter  $\epsilon_\nu^i \equiv r_{min}^i / r_{max}^i$  of the  $i$ -th hot spot at threshold  $\nu$  is found as follows: first, the center of the spot is estimated as the point with  $x_c, y_c$  coordinates equal to the mean of all the  $x$  and  $y$  coordinates of the pixels that form the spot respectively; second, the distance from this center point to all the pixels that lay on the boundary of the spot are calculated;  $r_{max}^i$  and  $r_{min}^i$  are the largest and shortest of these distances. The above mentioned procedure is repeated for several threshold levels ( $\nu : 1.0 - 3.0$  in steps of  $\Delta\nu = 0.25$ ). The geometric descriptor  $\epsilon_\nu$  used to measure the elongation of anisotropy spots at threshold  $\nu$  is the average of all the  $\epsilon_\nu^i$  at a fixed  $\nu$ .

At this point one can question whether the defined  $\epsilon_\nu$  really corresponds to the theoretical parameter of elongation in Fig. 1.

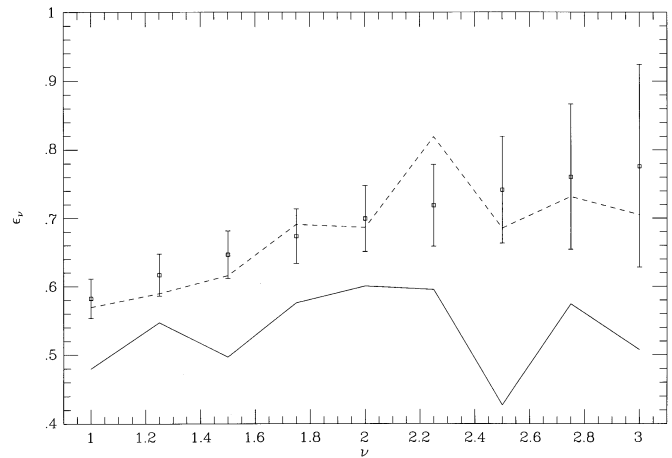


**Fig. 2.** Measured eccentricity parameter  $\epsilon_\nu$  for the COBE sum maps (solid) and difference maps (dash) compared with the expected eccentricity for noise Monte Carlo realizations (points with error bars).

The correspondence of the Lyapunov numbers or KS-entropy with parameters observed either with experiments or computer simulations is an essential problem. However, it has been empirically established that a correspondence with macroscopic parameters does exist (at least qualitative) and just this fact determines the role of those parameters as important tools for the study of nonlinear phenomena (Hilborn 1994 and references therein). Another question is whether the specific procedure of estimation of the mean elongation of spots can be crucial or not. Obviously other algorithms in principle can lead to numerically not absolutely equivalent results, but a drastic change of the situation seems unlikely, especially at high thresholds (Sommerer & Ott 1993 and references therein).

Fig. 2 shows  $\epsilon_\nu$  for the sum and difference DMR maps for threshold levels in the range  $\nu : 1.0 - 3.0$ . Data for  $\nu < 1.0$  is dominated by noise and for  $\nu > 3.0$  is limited by the large statistical error due to the small number of spots at high thresholds.

### 4. Results

The signature of the mixing of geodesics effect is a clear one: hot spots should have a fixed eccentricity independent of threshold level, and if these hot spots are elongated it is an indication of mixing in open spaces. In principle it is possible to detect eccentricities smaller than 1, the problem however is to disentangle the effect due to mixing from instrumental noise which by its stochastic nature is expected to produce anisotropy spots with certain degree of elongation.

In order to evaluate the statistical significance of a possible detection of the mixing of geodesics effect we have performed Monte Carlo studies of noise maps that take into account instrumental noise, COBE's sky coverage and pixelization. Noise maps were generated by assigning to each pixel on the map a temperature equal to a random number extracted from a Gaussian distribution with dispersion  $\sigma = \sigma_1 / \sqrt{N}$ , where  $\sigma_1$  is the

**Table 1.** Eccentricity parameter of hot spots on COBE maps ( $\epsilon_\nu^{A+B}$ ,  $\epsilon_\nu^{A-B}$ ) and comparison with Monte Carlo noise maps ( $\epsilon_\nu^{MC}$ ).  $\Delta^{A+B}$  and  $\Delta^{A-B}$  denote the difference (in standard deviations) between the measured eccentricities and the mean eccentricity of noise Monte Carlo maps.

$\nu$	$\epsilon_\nu^{A+B}$	$\epsilon_\nu^{A-B}$	$\epsilon_\nu^{MC}$	$\Delta^{A+B}$	$\Delta^{A-B}$
1.00	0.480	0.570	0.582	3.551	0.447
1.25	0.547	0.590	0.617	2.271	0.886
1.50	0.497	0.616	0.646	4.288	0.881
1.75	0.576	0.691	0.674	2.432	-0.429
2.00	0.600	0.686	0.699	2.049	0.267
2.25	0.595	0.819	0.719	2.060	-1.675
2.50	0.427	0.685	0.741	4.017	0.719
2.75	0.574	0.732	0.761	1.752	0.272
3.00	0.507	0.705	0.776	1.815	0.480

corresponding sensitivity for one observation and  $N$  the number of observations.

Maps for both  $A$  and  $B$  channels were generated independently. A difference map was formed and Gaussian smoothed just as it is done with the real data. The same algorithm used to obtain the eccentricity parameter of the COBE maps was used for each one of the Monte Carlo noise realizations. Fig. 2 shows the Monte Carlo mean eccentricity and the  $1-\sigma$  error bars expected from noise maps. Knowing the eccentricity expected from noise, one can estimate the probability that the observed eccentricity parameter can be produced by noise alone. Table 1 gives  $\epsilon_\nu$  for the COBE sum and difference maps, and the deviations from the mean eccentricity of Monte Carlo noise simulations.

The  $\chi^2$  statistic computed with the 9 data points in the range  $\nu = 1.0 - 3.0$  and the corresponding noise Monte Carlo points is 5.6 and 73.0 for the  $(A - B)$  and  $(A + B)$  maps respectively. The low  $\chi^2$  associated with the difference maps was expected and is an indication of the accuracy of the Monte Carlo simulations. On the other hand, the high  $\chi^2$  obtained when the data from the signal maps is compared with noise data is a clear indication of an actual detection of elongated anisotropy spots. The measured eccentricity parameter at threshold levels 1.5 and 2.5 in particular exhibit a  $> 4-\sigma$  deviation with respect to noise. The average deviation in terms of standard deviations of  $\epsilon_\nu^{A+B}$  from the corresponding Monte Carlo result for the 9 bins considered here is  $3\sigma$ . From the mixing of geodesics effect one would expect a constant eccentricity for all threshold levels. Due to the large dispersion of the measured  $\epsilon_\nu$  values it is not possible to make a strong statement in favor of the hypothesis of a constant  $\epsilon_\nu$  independent of  $\nu$ . However, it is seen that the contribution to the  $\chi^2$  is roughly the same independent of  $\nu$ . Under the hypothesis of a positive detection of elongated anisotropy spots and using the 9 points in Table 1, the measured eccentricity is  $\epsilon = 0.53 \pm 0.06$ .

## 5. Discussion

An excess elongation as possible genuine feature of the hot spots on COBE maps is well established at least at threshold levels  $\nu$  between 1.0 and 3.0. The detected excess elongation shows a statistically strong independence on the threshold, contrary to the case for the difference  $(A - B)$  maps where  $\epsilon_\nu$  shows a clear correlation with threshold. This characteristic dependence of the eccentricity parameter with threshold for noise maps is clearly manifest in Monte Carlo noise realizations. If the detection of high eccentricity of hot spots is attributed to the effect of mixing of geodesics flow, our analysis implies  $\Omega < 1$ . However one must also consider the fact that the detected effect can be produced in part by galactic contamination of the maps.

The numerical value of the obtained elongation parameter might have been obviously affected by a number of effects of cosmological and non-cosmological nature. Primordial fluctuations on the surface of last scattering, for example, would also produce non-zero ellipticity even in flat universe (Bond & Efstathiou 1987). However, due to the stochastic nature of this effect, the dependence of the ellipticity parameter with threshold would be just like that of noise, contrary to what we have observed (i.e. a threshold independent eccentricity). More statistics and higher accuracy is necessary for a reliable numerical evaluation of  $\Omega$ . A question thus arises as to how can one distinguish whether the observed elongation is really due to the effect of geodesics mixing? Indeed, although the “geodesics mixing” has put forward the idea of looking for the *threshold independent* elongation of hot spots on CMB sky maps as a signature for  $\Omega < 1$ , there are other mentioned effects that can be considered as well. Thus, to answer the question posed above it is important to have a thorough consideration of other observable consequences of the effect of mixing geodesics. As it is mentioned above, among those consequences is the decrease of the amplitude of initial fluctuations during the expansion of the Universe; the expected decrease depends on the curvature, the value of  $\Omega$  and the time of last scattering (Gurzadyan & Kocharyan 1992).

More interesting, however, can be the property concerning the dependence of the temperature autocorrelation function  $C(\theta, \beta)$  on the sky angle  $\theta$  with a beam size  $\beta$ . It was shown (Gurzadyan & Kocharyan 1996), that in negatively curved spaces  $C(\theta, \beta)$  tends to become constant with respect to  $\theta$  (i.e. independent on the sky angle) independent of the initial perturbation spectrum, but should depend on the beam size  $\beta$  by the asymptotic law

$$\frac{C(\theta, \beta)}{T^2} - 1 \sim \frac{\text{const}}{\beta}.$$

In other words, the observation with different beam sizes should lead to different values for the amplitude of the CMB anisotropy, namely the measured anisotropy decreases with increasing beam size.

Regarding the latter effect, note that some measurements by smaller beam sizes (Netterfield et al 1995; Ruhl et al 1995) seem to indicate higher values for the anisotropy amplitude as compared with the COBE data, even though one has to distinguish

the contributions of other effects such as the Doppler peak for example.

The peculiar feature of the effect of geodesic is its crucial dependence on the curvature of the Universe, i.e. its disappearance in flat and positively curved spaces, and independence on various models of dark matter or the spectrum of initial perturbations, etc.

Obviously nothing is happening to an individual photon during the free propagation after the last scattering epoch, and these effects are entirely statistical and determined by the principal limitations of obtaining information during the measurements, i.e. by the impossibility of the reconstruction of the trajectory of the photon while observing within finite smoothing angle and time period, due to the overlapping of exponentially deviating geodesics in any given cut of phase space (for detailed discussion of this and similar problems see Gurzadyan & Kocharyan 1994). Note that these effects differ from those of classical chaotic Mixmaster models, and can be alternatives to inflationary scenarios (Gurzadyan & Kocharyan 1994; Cornish et al. 1996). The measured effect of elongation of anisotropy spots in CMB sky maps can be the direct footprint of the negative curvature of the Universe and therefore has a considerable impact on cosmology.

*Acknowledgements.* The authors would like to thank R.Juszkievicz, A.Kocharyan and R.Ruffini for valuable discussions of the results. One of us (V.G.) is thankful to R.Penrose for the discussion of the geometrical aspect of the effect of geodesics mixing. This research is in part funded by COLCIENCIAS of Colombia (2228-05-091-95) and The Royal Society. The COBE datasets were developed by the NASA Goddard Space flight Center under the guidance of the COBE Science Working Group and were provided by the NSSDC.

## References

- Adler, R. J. 1981, *The Geometry of Random Fields*, (Chichester: Wiley)
- Arnold, V.I. 1989, *Mathematical Methods of Classical Mechanics*, Nauka, Moscow
- Bennett, C. L., et al. 1994, ApJ, 436, 423
- Bennett, C. L., et al. 1996, ApJ, 464, L1
- Bond, J.R. & Efstathiou, G. 1987, MNRAS, 226, 655
- Cayón, L. & Smoot, G. F. 1995, ApJ, 452, 487
- Coles, P. 1988, MNRAS, 234, 509
- Cornish N.J., Spergel D.N. & Starkman G.D. 1996, Phys. Rev. Lett., 77, 215
- De Gouveia, E. M., et al. 1995, ApJ, 442, L45
- Ellis G., Tavakol R. 1994, Class.Quant.Grav., 11, 675
- Fabbri, R. & Torres, S. 1995, Nuovo Cimento, 110B, 865
- Fabbri, R. & Torres, S. 1996, A&A, 307, 703
- Ganga, K., Cheng, E., Meyer, S. & Page, L. 1993, ApJ, 410, L57
- Gott, J. R. et al. 1990, ApJ, 352, 1
- Gurzadyan V.G. & Kocharyan, A.A. 1991, in: *Quantum Gravity, V*, (eds Berezin V.A., Markov M.A. & Frolov V.P.) p.689 (World Sci. Singapore).
- Gurzadyan, V.G. & Kocharyan, A.A. 1992, A&A, 260, 14
- Gurzadyan, V.G. & Kocharyan, A.A. 1993a, Int. Journ. Mod. Phys. D., 2, 97
- Gurzadyan, V.G. & Kocharyan, A.A. 1993b, Europhys. Lett. 22, 231

- Gurzadyan V.G. & Kocharyan, A.A. 1996, in: *Quantum Gravity, VI*, (eds Berezin V.A., & Rubakov V.A.) (World Sci. Singapore, in press); ICTP Preprint IC/93/419, Trieste, 1993
- Gurzadyan, V.G. & Kocharyan, A.A. 1994, *Paradigms of the Large-Scale Universe*, (Gordon and Breach, New York).
- Gurzadyan, V.G., & Margarian, A. 1996, Physica Scripta, 53, 513
- Gurzadyan, V.G. & Torres, S. 1993, in: *Present and Future of the Cosmic Microwave Background*, (Eds. J.L. Sanz, et al.) 429, p.139 (Heidelberg: Springer-Verlag)
- Hancock, S., et al. 1994, Nature, 367, 333
- Hilborn, R.C. 1994, *Chaos and Nonlinear Dynamics*, (Oxford University Press, Oxford).
- Kogut, et al. 1996, ApJ, 464, L29
- Martínez-González, E., Cayón, L. 1992, in *The Infrared and Submillimetre Sky after COBE* (eds M. Signore and C. Dupraz) 303 (Netherlands: Kluwer Academic Press)
- Martínez-González, E. & Sanz, J. L. 1989, MNRAS, 237, 939
- Naselsky, P. D., & Novikov, D. I. 1995, ApJ, 444, L1
- Netterfield, C.B., et al. 1995, ApJ, 445, L69
- Ruhl J.E., et al. 1995, ApJ, 453, L1
- Sazhin, M. V. 1985, MNRAS, 216, 25p
- Smoot, G.F., et al. 1990, ApJ, 360, 685
- Smoot, G. F., et al. 1992, ApJ, 396, L1
- Smoot, G. F., et al. 1994, ApJ, 437, 1
- Sommerer, J.C., & Ott, E. 1993, Science, 259, 335
- Torres, S., et al. 1989, in *Data Analysis in Astronomy III* (eds V. di Gesu, L. Scarsi, and M.C. Maccarone) 319 (New York: Plenum)
- Torres, S. 1994, ApJ, 423, L9
- Torres, S., et al. 1995, MNRAS, 274, 853
- Torres, S. 1995a, Astro. Lett. and Communications, 32, 95
- Torres, S. 1995b, Astrophys. and Space Sci. 228, 313
- Vittorio, N. & Juszkievicz, R. 1987, ApJ, 314, L29
- White, M., Scott, D. & Silk, J. 1994, Ann.Rev.A & A, 32, 319